Chemical pressure effect on the transport and electronic band structure of $Fe_2V_{1-x}Nb_xAl$

C. S. Lue, R. F. Liu, and M. Y. Song
Department of Physics, National Cheng Kung University, Tainan 70101, Taiwan

K. K. Wu and Y. K. Kuo*
Department of Physics, National Dong Hwa University, Hualien 97401, Taiwan

(Received 11 June 2008; revised manuscript received 2 September 2008; published 17 October 2008)

We report the effects of partial substitution of Nb onto the V sites of Fe_2VAl by measuring the electrical resistivity, Seebeck coefficient, and thermal conductivity as a function of temperature. It is found that the Nb substitution effectively produces a negative chemical pressure in the system. As a result, the Nb-substituted materials show enhanced semiconductinglike behavior in their electrical resistivity. In addition, the Seebeck coefficient changes sign from positive to negative while replacing V with Nb. These phenomena have been associated with the change of the band features, mainly due to the decrease in the number of the hole carriers. To identify this scenario, we performed *ab initio* calculations to investigate the electronic band structures of $Fe_2V_{1-x}Nb_xAl$, focusing on the band variation around the Fermi level. Theoretical results indicate a significant reduction in the hole pockets through Nb substitution, which is consistent with experimental observations.

DOI: 10.1103/PhysRevB.78.165117 PACS number(s): 72.15.Eb, 72.15.Jf, 71.20.Be

I. INTRODUCTION

Heusler-type intermetallics with a general formula X_2YZ (where X and Y are transition metals and Z is often an element from columns III through VI in the periodic table) have attracted considerable attention because of their various transport and magnetic features. Semiconductors, semimetals, normal Pauli metals, weak ferromagnets, antiferromagnets, as well as half-metallic ferromagnets exist in this class of materials. Fe_2VAl, a material of this prototype, has been characterized as a nonmagnetic semimetal from intense experimental and theoretical researches.[1–12] The semimetallic nature of Fe_2VAl has been attributed to the presence of a pseudogap around the Fermi level, arising from a slightly indirect overlap between the electron and hole pockets.[7–11] The exotic behavior observed in the electrical resistivity, the nuclear-magnetic-resonance (NMR) Knight shift, and the spin-lattice relaxation rate have been associated with the thermally excited quasiparticles across the pseudogap.[1,2] An optical-conductivity study on Fe_2VAl has further confirmed the existence of a pseudogap in the vicinity of the Fermi level.[3]

Theoretical calculations have indicated that the pseudogap in Fe_2VAl will open to a real gap if the volume is expanded by about 6%.[10] Fe_2NbAl, an artificial Heusler compound with a larger lattice constant, was thus predicted to be a semiconductor with a gap of about 0.2 eV.[10] While a real sample of Fe_2NbAl does not exist, the partial substitution of Nb atoms onto the V sites of Fe_2VAl yielding a series of $Fe_2V_{1-x}Nb_xAl$ compounds may be achieved. Since the niobium atom is isoelectronic to the vanadium and has a larger atomic radius, the substitution would cause a lattice expansion, which is an effectively negative chemical pressure in Fe_2VAl. With this regard, it allows us to study the evolution of electronic band structures by the chemical pressure effect.

In this work, we performed a detailed transport investigation by means of the electrical resistivity, the Seebeck coefficient, as well as the thermal-conductivity measurements on $Fe_2V_{1-x}Nb_xAl$ with x ranging from 0 to 0.1. It is known that Seebeck coefficient is very sensitive to the electronic band features near the Fermi surfaces, and the results can be used to interpret the change of the band structures through Nb substitution. In a parallel study, *ab initio* calculations were also employed to investigate the electronic band structures of $Fe_2V_{1-x}Nb_xAl$, focusing on the features around the Fermi level. Theoretical results indicate that the Nb substitution has an effect that reduces the hole pockets in the vicinity of the Fermi level, which is consistent with experimental observations.

II. EXPERIMENTAL DETAILS

Polycrystalline $Fe_2V_{1-x}Nb_xAl$ (x=0, 0.03, 0.06, and 0.1) samples were prepared by an ordinary arc-melting technique. Briefly, a mixture of appropriate amounts of high-purity elemental metals was placed in a water-cooled copper crucible and then melted several times in an argon flow arc melter. The weight loss during melting is less than 0.5% for each compound. To promote homogeneity, these ingots were annealed in a vacuum-sealed quartz tube at 800 °C for two days and followed by furnace cooling. This is a typical process that forms in a single-phase $L2_1$ (Heusler-type) structure.[13–17]

Room-temperature x-ray diffraction taken with Cu $K\alpha$ radiation on the powder $Fe_2V_{1-x}Nb_xAl$ specimens is identified to the expected $L2_1$ structure—a more detailed analysis of the x-ray data, in which the Heusler-type structure was refined with the Rietveld method. We thus obtained the lattice constant, a, for each composition with the variation as a function of x illustrated in Fig. 1. It clearly demonstrates that the lattice constant consistently increases as Fe_2VAl deviates from its stoichiometry, indicating that the V sites are successfully replaced by Nb atoms according to Vegard's law. It should be mentioned that a sample with the nominal composition of x=0.2 was also synthesized under the same preparation condition. The x-ray powder-diffraction pattern exhibits no expected $L2_1$ phase, suggesting that this substitution level is beyond the solubility limit for Nb in Fe_2VAl.

Electrical resistivity for the $Fe_2V_{1-x}Nb_xAl$ alloys was obtained by a standard dc four-terminal method. Seebeck coef-

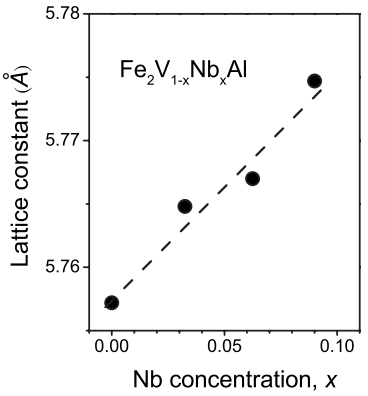

FIG. 1. Lattice constant versus Nb concentration as obtained from x-ray diffraction.

ficients were measured with a dc pulse technique. Seebeck voltages were detected using a pair of thin Cu wires electrically connected to the sample with silver paint at the same positions as the junction of differential thermocouple. The stray thermal emfs are eliminated by applying long current pulses ($\sim$100 s) to a chip resistor which serves as a heater, where the pulses appear in an off-on-off sequence.

Thermal-conductivity measurements were carried out in a closed-cycle refrigerator using a direct heat-pulse technique. All samples were cut to a rectangular parallelepiped shape with the typical size of $1.5\times1.5\times5.0$ mm^3. One end was glued (with thermal epoxy) to a copper block that served as a heat sink, while a calibrated chip resistor was connected to the other end as a heat source. The temperature difference was detected by using an *E*-type differential thermocouple with junctions thermally attached to two well-separated positions along the sample. The temperature difference was controlled to be less than 1 K to minimize the heat loss through thermal radiation, and the sample space is maintained in a good vacuum (approximately 1×10^{-4} torr) during measurements. All experiments were performed upon warming with a rate slower than 20 K/h. The uncertainty of our thermal conductivity is about 15%, mainly arising from the error on the determination of the geometrical factor of these samples.

III. RESULTS AND DISCUSSION

A. Electrical resistivity

In Fig. 2, we plot the temperature variation of the electrical resistivity $\rho(T)$ for $Fe_2V_{1-x}Nb_xAl$. It is apparent that all studied compositions show semiconducting behavior as indicated by their negative temperature coefficient of resistivity (TCR). However, these materials are still classified as semimetals because of their finite residual resistivity at low temperatures and nonzero Fermi-level density of states (DOS) revealed from theoretical calculations. With substituting Nb atoms onto the V sites, the residual electrical resistivity gradually increases, showing enhanced semiconductinglike behavior. Such an observation is attributed to a decrease in the number of carriers responsible for the electrical transport. This is mainly due to the reduction in the hole pockets at the

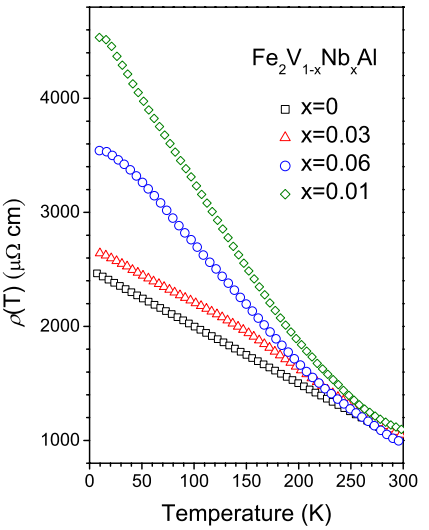

FIG. 2. (Color online) Electrical resistivity $\rho(T)$ as a function of temperature for $Fe_2V_{1-x}Nb_xAl$.

Γ point via Nb substitution in accordance with the band-structure calculations in $Fe_2V_{1-x}Nb_xAl$. A detailed interpretation will be given in the theoretical section.

B. Seebeck coefficient

The temperature-dependent Seebeck coefficient of $Fe_2V_{1-x}Nb_xAl$ is shown in Fig. 3. For the stoichiometric compound, the measured *S* is found to be positive in the entire temperature range we investigated. Such a finding suggests that the dominant carrier for the transport is *p*-type in Fe_2VAl, which is consistent with the previous results.[18–21] This is also in good agreement with the band-structure calculations which revealed the existence of relative large hole pockets near the Fermi level in Fe_2VAl.[7–10] However, the small absolute value of *S* implies that the electrons and holes involved in the heat transport processes are nearly compensated. Hence, a slight variation in the carrier concentration

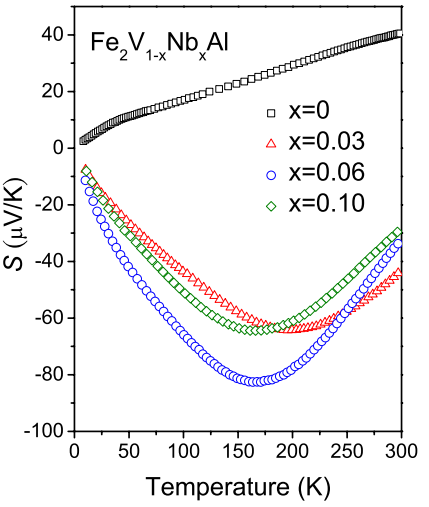

FIG. 3. (Color online) Seebeck coefficient vs temperature in $Fe_2V_{1-x}Nb_xAl$.

would change the type of the dominant carrier responsible for the observed Seebeck coefficient. In fact, by replacing V with Nb, the sign of S reverses, which can be realized as a decrease in the number of the p-type carriers arising from the reduction in the hole pockets. As a consequence, the electron pockets become comparatively larger and the associated n-type carriers thus govern the thermoelectric transport in these substituted materials.

For the Nb-substituted $Fe_2V_{1-x}Nb_xAl$ alloys, the Seebeck coefficient develops a broad minimum at intermediate temperatures, and the corresponding valley position shifts to lower temperatures while increasing Nb content. This trend can be qualitatively understood as the narrowing of the pseudogap, resulting in a lower activated energy for the hole carriers thermally excited across the corresponding pseudogap. After passing through the minimum, the slope of S changes from negative to positive which can be ascribed by the contribution of thermally excited opposite carriers across their pseudogaps. Similar features have been found in other semimetallic Heusler systems such as Fe_2VGa and Fe_2TiSn.[22,23] Upon heating, intrinsic electrons and holes are excited. If the holes have a slightly higher mobility than the electrons in these materials, the p-type carriers will eventually govern the thermal transport, leading to a more positive value in S at high temperatures.

It is worthwhile mentioning that the maximum absolute value of S is only about 80 μV/K in $Fe_2V_{0.94}Nb_{0.06}Al$ at around 170 K. This value is substantially lower than those reported in the Fe_2VAl-based alloys. For examples, the magnitude of S reaches 130 μV/K in $Fe_2VAl_{0.95}Si_{0.05}$, $Fe_2VAl_{0.95}Ge_{0.05}$, and $Fe_2VAl_{0.94}In_{0.06}$ near room temperature.[21,24–26] The observed small S values in the $Fe_2V_{1-x}Nb_xAl$ series should strongly depend on their electronic structures as the absolute value of S in ordinary metals is inversely proportional to the density of states, $N(E)$, and proportional to its energy derivative $\partial N(E)/\partial E$ around the Fermi level. On this basis, the relatively small $\partial N(E)/\partial E$ could be the significant factor leading to the low S values in $Fe_2V_{1-x}Nb_xAl$.

C. Thermal conductivity

In Fig. 4, we display the observed thermal conductivity for all studied $Fe_2V_{1-x}Nb_xAl$ samples. Generally, the total thermal conductivity for ordinary metals and semimetals is a sum of electronic and lattice terms. The electronic thermal conductivity (κ_e) can be evaluated using the Wiedemann-Franz law $\kappa_e\rho/T=L_o$, where ρ is the measured dc electric resistivity and $L_0=2.45\times10^{-8}$ WΩ K^{-2} is the Lorentz number. The lattice thermal conductivity (κ_L) is thus obtained by subtracting κ_e from the observed κ. This estimate gives a very small contribution of κ_e, suggesting that the thermal conductivity shown in Fig. 4 is essentially due to κ_L.

Between 50 and 80 K, κ_L develops a maximum which is a typical signature for the reduction in the phonon scattering in solids at low temperatures. A systematic trend found in κ_L is that the height of the low-temperature peak gradually decreases with increasing the substitution level, which is indicative of a strong enhancement in the phonon scattering by

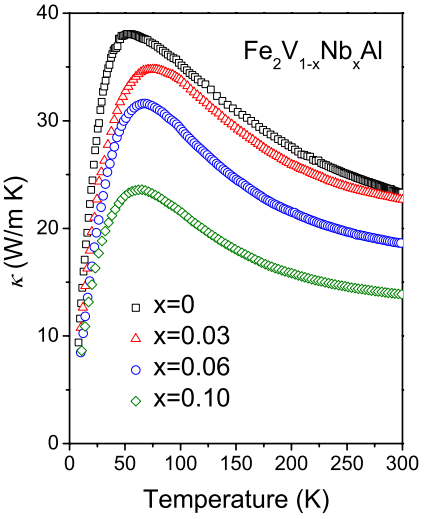

FIG. 4. (Color online) Temperature dependence of the observed thermal conductivity in $Fe_2V_{1-x}Nb_xAl$.

Nb substitution. It is worthwhile mentioning that such κ_L features in the semimetals of $Fe_2VAl_{1-x}Si_x$ and $Fe_2VGa_{1-x}Ge_x$ behave in a similar manner.[24,27] A detailed analysis of κ_L using the model of Debye approximation[28,29] further indicates that the point-defect scattering of the phonons plays an important role in the reduction in κ_L. We argue that these point defects originated from the mass fluctuation between V and Nb because their atomic mass difference is about 80%. It thus causes a marked drop in the low-temperature phonon peak for the Nb-substituted samples.

D. Calculated band structure of $Fe_2V_{1-x}Nb_xAl$

In order to substantiate our experimental perspectives and gain a further insight on the band structures of $Fe_2V_{1-x}Nb_xAl$, we performed first-principles calculations with substituted levels of $x=0$, 0.03125, 0.0625, 0.125, 0.25, 0.375, 0.5, and 1. Our calculations are within the framework of density-functional theory (DFT).[30] The exchange-correlation potential was treated locally under the generalized gradient approximation (GGA) proposed by Perdew.[31] The interaction between core and valence electrons was described by projector augmented-wave (PAW) method[32] implemented by Kresse and Joubert.[33] The one-electron Kohn-Sham wave functions were expanded by plane-wave basis with kinetic-energy cutoff of 267.9 eV. The numbers of treated valence electrons are 8, 5, 11, and 3 for Fe, V, Nb, and Al, respectively. The k-point sampling in the Brillouin zone (BZ) was constructed by the Monkhorst-Pack method.[34] All calculations are carried out using Vienna *ab initio* simulation package (VASP).[35–37]

The k-point set of (10 10 10) was used for the unit cell which consists of eight Fe atoms, four V atoms, and four Al atoms. The calculated lattice constants are 5.678 Å for Fe_2VAl and 5.905 Å for Fe_2NbAl, respectively. The same density of k-point set was further used for the supercells which are constructed by $2\times2\times2$ unit cells. With the same size of supercell, we replaced 1, 2, 4, 8, 12, and 16 V atoms with Nb atoms in order to simulate the systems with substi-

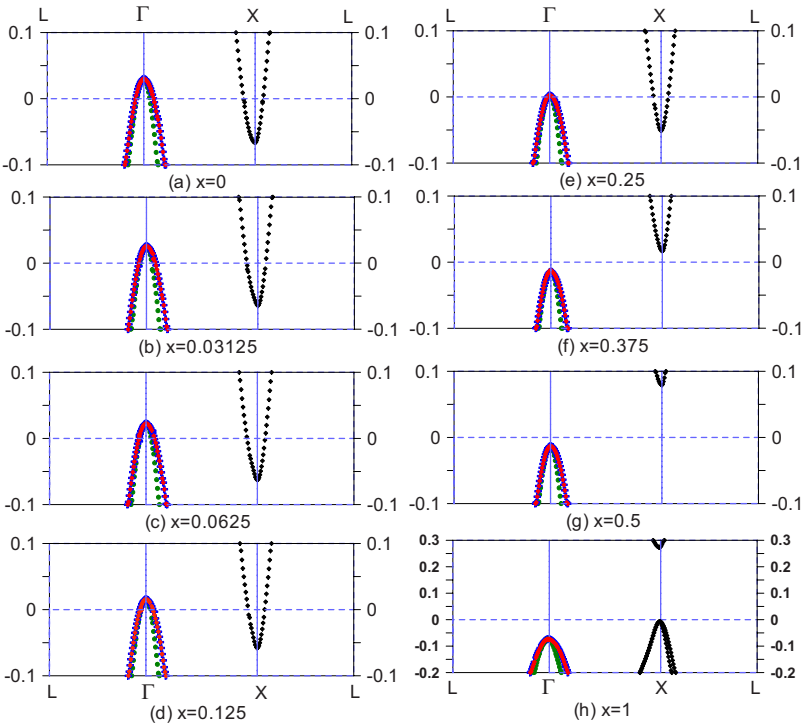

FIG. 5. (Color online) Enlargement of the band structures of $Fe_2V_{1-x}Nb_xAl$ for $x=0$, 0.03125, 0.0625, 0.125, 0.25, 0.375, 0.5, and 1. The Fermi level is denoted at zero.

tuted levels of $x=0.03125$, 0.0625, 0.125, 0.25, 0.375, and 0.5, respectively. The atomic forces in the supercell were relaxed by moving atoms to the positions at which all atomic forces are smaller than 0.02 eV/Å. The cell volume and shape were also allowed to relax. Comparing to the system without Nb doping, the lattice constant of the system with $x=0.5$, i.e., $Fe_{64}(V_{16}Nb_{16})Al_{32}$, is found to expand by 2.1%. The band structures were then calculated from the supercells with equilibrium ground-state structures.

Figure 5 presents the results of band structures along symmetry lines L-Γ-X-L for the substituted levels of $x=0$, 0.03125, 0.0625, 0.125, 0.25, 0.375, 0.5, and 1. Note that the energy range is given from −0.2 to 0.3 eV for $x=1$ (Fe_2NbAl). It is clearly seen from Figs. 5(a)–5(h) that the band structures of Fe_2VAl are significantly modified upon Nb substitutions, i.e., from semimetallic for V-rich compounds to insulating when about 37% of V content is replaced by Nb atoms.[38] The formation of a band gap in Fe_2NbAl revealed from our calculation is consistent with the previous result calculated by Weinert and Watson.[10] The hole bands along L-Γ-X in Fig. 5 are indicated by three different symbols, i.e., blue crosses, red diamonds, and green dots. It is shown that the three hole bands consist of one twofold degeneracy as well as one singlet. With the addition of Nb atoms in the system, the population of the hole carriers above the Fermi energy gradually decreases while increasing the Nb content in $Fe_2V_{1-x}Nb_xAl$.

We thus have a concise picture for the band-structure variation of $Fe_2V_{1-x}Nb_xAl$. While replacing V with Nb atoms, the lattice constant gradually increases, which is equivalent to the application of a negative pressure on the system. This will cause a downward shift of the hole pockets but has little effect on the electron ones. As a result, the indirect overlap between the electron and hole pockets reduces, leading to a more semiconductinglike characteristic in their electrical resistivity. This scenario is also consistent with the observation of the Seebeck coefficient. As the hole pockets become smaller, the electrons turn into the dominant carriers for the thermoelectric transport, resulting in the observed sign reversal in S for the studied $Fe_2V_{1-x}Nb_xAl$ alloys with $x\neq 0$.

IV. CONCLUSIONS

In summary, we have investigated the effect of the Nb substitution on the thermal transport and band structures of $Fe_2V_{1-x}Nb_xAl$. The substitution of large Nb atoms onto the V sites consistently causes the lattice expansion. This is equivalent to the production of a negative chemical pressure in the system, resulting in a significant reduction in hole pockets as revealed from *ab initio* calculations. Agreement is obtained for the theoretical prediction as compared to the results of the electrical resistivity and the Seebeck coefficient for $Fe_2V_{1-x}Nb_xAl$. The conclusion made in this study provides a concise understanding of the evolution of band structures in $Fe_2V_{1-x}Nb_xAl$ via lattice expansion. Furthermore, the observed tendency should be relevant to other semimetallic Heusler-type materials that will undergo a semimetal-insulator transition if a real compound with a larger lattice constant exists.

ACKNOWLEDGMENTS

This work was supported by the National Science Council of Taiwan under Grants No. NSC-95-2112-M-006-021-MY3 (C.S.L) and No. NSC-96-2112-M-259-003 (Y.K.K). We acknowledge useful conversations with C. Cheng of National Cheng Kung University for the details of the first-principles calculations.

*ykkuo@mail.ndhu.edu.tw

[1] Y. Nishino, M. Kato, S. Asano, K. Soda, M. Hayasaki, and U. Mizutani, Phys. Rev. Lett. **79**, 1909 (1997).
[2] C. S. Lue and J. H. Ross, Jr., Phys. Rev. B **58**, 9763 (1998); **61**, 9863 (2000).
[3] H. Okamura, J. Kawahara, T. Nanba, S. Kimura, K. Soda, U. Mizutani, Y. Nishino, M. Kato, I. Shimoyama, H. Miura, K. Fukui, K. Nakagawa, H. Nakagawa, and T. Kinoshita, Phys. Rev. Lett. **84**, 3674 (2000).
[4] Y. Nishino, Mater. Trans. **42**, 902 (2001).
[5] A. Matsushita, T. Naka, Y. Takano, T. Takeuchi, T. Shishido, and Y. Yamada, Phys. Rev. B **65**, 075204 (2002).
[6] Y. Nishino, H. Sumi, and U. Mizutani, Phys. Rev. B **71**, 094425 (2005).
[7] G. Y. Guo, G. A. Botton, and Y. Nishino, J. Phys.: Condens. Matter **10**, L119 (1998).
[8] D. J. Singh and I. I. Mazin, Phys. Rev. B **57**, 14352 (1998).
[9] R. Weht and W. E. Pickett, Phys. Rev. B **58**, 6855 (1998).
[10] M. Weinert and R. E. Watson, Phys. Rev. B **58**, 9732 (1998).
[11] A. Bansil, S. Kaprzyk, P. E. Mijnarends, and J. Tobola, Phys. Rev. B **60**, 13396 (1999).
[12] V. N. Antonov, A. Ernst, I. V. Maznichenko, A. N. Yaresko, and A. P. Shpak, Phys. Rev. B **77**, 134444 (2008).
[13] Y. Feng, J. Y. Rhee, T. A. Wiener, D. W. Lynch, B. E. Hubbard, A. J. Sievers, D. L. Schlagel, T. A. Lograsso, and L. L. Miller, Phys. Rev. B **63**, 165109 (2001).
[14] I. Maksimov, D. Baabe, H. H. Klauss, F. J. Litterst, R. Feyerherm, D. M. Tobbens, A. Matsushita, and S. Sullow, J. Phys.: Condens. Matter **13**, 5487 (2001).
[15] C. S. Lue, Yang Li, Joseph H. Ross, Jr., and George M. Irwin, Phys. Rev. B **67**, 224425 (2003).
[16] C. S. Lue, Y. K. Kuo, S. N. Hong, S. Y. Peng, and C. Cheng, Phys. Rev. B **71**, 064202 (2005).
[17] A. Ślebarski, J. Goraus, J. Deniszczyk, and Ł. Skoczeń, J. Phys.: Condens. Matter **18**, 10319 (2006).
[18] H. Kato, M. Kato, Y. Nishino, U. Mizutani, and S. Asano, J. Jpn. Inst. Met. **65**, 652 (2001).
[19] Y. Nishino, H. Kato, M. Kato, and U. Mizutani, Phys. Rev. B **63**, 233303 (2001).
[20] C. S. Lue and Y.-K. Kuo, Phys. Rev. B **66**, 085121 (2002).
[21] Y. Nishino, Mater. Sci. Forum **449-452**, 909 (2004).
[22] C. S. Lue, W. J. Lai, C. C. Chen, and Y.-K. Kuo, J. Phys.: Condens. Matter **16**, 4283 (2004).
[23] C. S. Lue and Y. K. Kuo, J. Appl. Phys. **96**, 2681 (2004).
[24] C. S. Lue, C. F. Chen, J. Y. Lin, Y. T. Yu, and Y.-K. Kuo, Phys. Rev. B **75**, 064204 (2007).
[25] Y. Nishino, S. Deguchi, and U. Mizutani, Phys. Rev. B **74**, 115115 (2006).
[26] M. Vasundhara, V. Srinivas, and V. V. Rao, Phys. Rev. B **77**, 224415 (2008).
[27] C. S. Lue, J. W. Huang, D. S. Tsai, K. M. Sivakumar, and Y.-K. Kuo, J. Phys.: Condens. Matter **20**, 255233 (2008).
[28] J. Callaway, Phys. Rev. **113**, 1046 (1959).
[29] J. Callaway and H. C. von Baeyer, Phys. Rev. **120**, 1149 (1960).
[30] P. Hohenberg and W. Kohn, Phys. Rev. **136**, B864 (1964); W. Kohn and L. J. Sham, *ibid.* **140**, A1133 (1965).
[31] J. P. Perdew, in *Electronic Structure of Solids '91*, edited by P. Ziesche and H. Eschrig (Akademie-Verlag, Berlin, 1991).
[32] P. E. Blöchl, Phys. Rev. B **50**, 17953 (1994).
[33] G. Kresse and D. Joubert, Phys. Rev. B **59**, 1758 (1999).
[34] H. J. Monkhorst and J. D. Pack, Phys. Rev. B **13**, 5188 (1976).
[35] G. Kresse and J. Hafner, Phys. Rev. B **47**, 558 (1993); **49**, 14251 (1994).
[36] G. Kresse and J. Furthmuller, Comput. Mater. Sci. **6**, 15 (1996).
[37] G. Kresse and J. Furthmuller, Phys. Rev. B **54**, 11169 (1996).
[38] For $x=0.375$, depending on the arrangements of 12 substituting Nb atoms in the $2\times2\times2$ supercell, the shape of the relaxed structure could change. The relaxed cell for which the band structure presented in Fig. 5(f) is found to be simple monoclinic and to expand in volume by 4.88%. Although the band structure displays an indirect band gap between Γ and X points, further analysis from total density of states indicates that it remains semimetallic. We had constructed several different relaxed structures for $x=0.375$ and found that the gap could be opened. However, the tendency of the decreasing hole carriers is consistently observed.